Progress in Oceanography 202 (2022) 102761

Contents lists available at ScienceDirect

Progress in Oceanography

journal homepage: www.elsevier.com/locate/pocean

Transportation and predation control structures the distribution of a key calanoid in the Nordic Seas

Johanna M. Aarflot [a,*], Solfrid S. Hjøllo [a], Espen Strand [b], Morten D. Skogen [a]

[a] Ecosystem Processes Group, Institute of Marine Research, Pb.1870, N-5817 Bergen, Norway
[b] Plankton Group, Institute of Marine Research, Pb.1870, N-5817 Bergen, Norway

ARTICLE INFO

Keywords:
Ecological model
Environmental control
Life-history variation
NORWECOM.E2E
ODD
Temperature-dependent growth
Top-down population control
Zooplankton transportation

ABSTRACT

The largest *Calanus* species in the Nordic Seas is also the copepod for which we have the poorest knowledge. Recent studies have shown that *C. hyperboreus* is more likely of sub-Arctic rather than Arctic origins, and the Nordic Seas are part of its core distribution areas worldwide. Large size and high fat content makes *C. hyperboreus* important prey for planktivores, and the Nordic Seas serve as main feeding grounds for a considerable biomass of planktivorous fish. We develop an individual-based model (IBM) based on existing knowledge of growth and life history of *C. hyperboreus*, and couple the IBM to an ecosystem model system encompassing physics, a nutrients–phytoplankton–zooplankton–detritus (NPZD) model and an IBM of the Atlantic congener *C. finmarchicus*. Given the main circulation routes in the region, a key question we address in this study is why *C. hyperboreus* is measured in low abundances in the (presumably) more favourable Norwegian Sea environment. We show that a core population of *C. hyperboreus* in the Greenland Sea supplies individuals to both the Iceland and Norwegian Seas, and that most copepods will visit more than one of the three regions during their life time. Advective pathways through environmental gradients creates intraspecific variation in development rates as reported by *in situ* observational studies. Furthermore, our results suggest that low abundances in the Norwegian Sea are more likely controlled by top-down processes (predation) rather than environmental limitations on growth or resource competition with *C. finmarchicus*.

1. Introduction

With its large size, *Calanus hyperboreus* is easily distinguished from other calanoids when analysing zooplankton samples with a microscope. It is one of four *Calanus* species present in the Nordic Seas (Greenland, Iceland and Norwegian Sea, Fig. 1) where we also find its congeners *C. finmarchicus*, *C. glacialis* and *C. helgolandicus* (Conover, 1988; Strand et al., 2020). Around 20 million tonnes of pelagic, planktivorous fish utilize the Nordic Seas as main foraging grounds (ICES, 2020) and feed on calanoid copepods (Bachiller et al., 2016). Larger body size means that *C. hyperboreus* has a greater total lipid content than its congeners (Renaud et al., 2018), making it an important prey source supporting high growth rates for fish (van Deurs et al., 2015). Still, the current knowledge on the spatial distribution and population dynamics of *C. hyperboreus* in this region of economically important fisheries is based on few sources (Broms et al., 2009), and the structuring mechanisms remain unclear.

C. hyperboreus is generally referred to as an Arctic copepod (e.g. Falk-Petersen et al., 2009) and has some key characteristics that facilitates survival despite highly unpredictable food supply, a feature characteristic of Arctic marine ecosystems. It may overwinter as early as copepodite stage C3 (Østvedt, 1955; Ashjian et al., 2003), and spends up to 4 years or more to complete a life cycle (Hirche, 1997; Falk-Petersen et al., 2009). Both egg production and survival through the first nauplii stages are not dependent on external food sources but fuelled by lipid reserves in the adult and eggs, respectively (Niehoff et al., 2002; Jung-Madsen et al., 2013). Eggs laid by female *C. hyperboreus* are larger and more lipid-rich than eggs from the other calanoids (Jung-Madsen et al., 2013). Furthermore, experimental studies have suggested that female *C. hyperboreus* may be capable of spawning during successive years (Plourde et al., 2003; Hirche, 2013), which is considered a unique trait amongst the *Calanus* species and presumably enhances the chance of successful recruitment.

Conover (1988) described *C. hyperboreus* as an Arctic endemic, and suggested that its presence in sub-Arctic regions was a result of expatriation; the large size and energy reserves would aid survival during expatriation, leading to longer transportation distances compared to other Arctic zooplankton. Later, the Greenland Sea has been pointed

* Corresponding author.
E-mail addresses: johanna.aarflot@hi.no (J.M. Aarflot), solfrid.hjollo@hi.no (S.S. Hjøllo), espen.strand@hi.no (E. Strand), morten.skogen@hi.no (M.D. Skogen).

https://doi.org/10.1016/j.pocean.2022.102761
Received 23 June 2021; Received in revised form 12 November 2021; Accepted 8 February 2022
Available online 26 February 2022

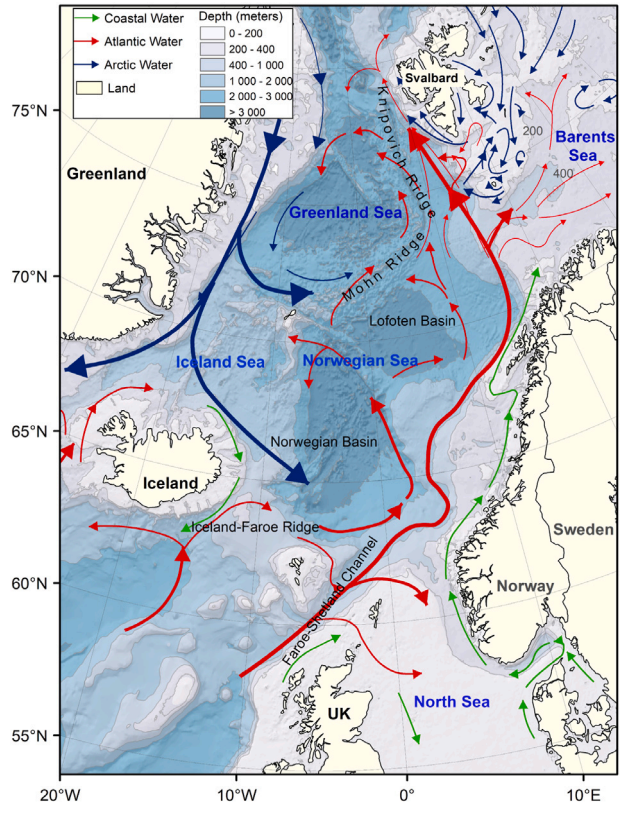

Fig. 1. Map of the Nordic (Greenland, Iceland and Norwegian) Seas and adjacent regions, with bottom topography and main circulation features.

to as a core overwintering area supplying individuals transported both southwards into the Iceland and Norwegian Seas and northwards to the Arctic Ocean (Hirche, 1991, 1997). Recent data compilations have demonstrated that this species is in fact more abundant in sub-Arctic than in Arctic regions, and indicates that *C. hyperboreus* is an expatriate rather than endemic species to the Arctic (Kvile et al., 2018). In the Nordic Seas, *C. hyperboreus* is often associated with Arctic waters (e.g. Astthorsson and Gislason, 2003; Broms et al., 2009; Strand et al., 2020). It may dominate in biomass both in the Iceland (Astthorsson and Gislason, 2003) and Greenland Seas, in the latter it has been observed in dense aggregations as deep as 2500 m (Hirche et al., 2006). The presence in the Norwegian Sea is considered negligible (Broms et al., 2009), though it has been found to coexist with other *Calanus* species in Norwegian fjords (Choquet et al., 2017).

Copepods drift with the ocean currents, and core populations must be upheld by circulation loops or similar advective forces that enable life cycle closure within a specific area. The Greenland Sea Gyre is presumably key for maintaining a core population of *C. hyperboreus* in the Greenland Sea (Falk-Petersen et al., 2009). Nevertheless, it must exit this gyre to distribute further south into the Iceland Sea. Given the long life cycle (3–6 years) and dominating current regimes in the Nordic Seas (Mork and Blindheim, 2000; Aksnes and Blindheim, 1996) (Fig. 1) one should perhaps expect a higher abundance of *C. hyperboreus* also in the Norwegian Sea. Why this species is observed in low abundances here compared to other regions in the Nordic Seas is a key question we address in this study. Low abundances in the Norwegian Sea have earlier been ascribed to expatriation from the Greenland Sea Gyre (Carstensen et al., 2012) and premature recruitment in relation to the spring bloom leading to unsuccessful reproduction in warm Atlantic water (Broms et al., 2009). Historic observations from Weather Station M (66°N, 2°E) did nevertheless demonstrate reproductive activity by *C. hyperboreus* here (Østvedt, 1955).

Modelling is a useful tool for studying the complex dynamics between zooplankton and their environment (e.g. Dorman et al., 2015; Xu et al., 2015; Stillman et al., 2015), and individual-based models (IBMs) allow explicit inclusion of individual variation in the model population (DeAngelis and Mooij, 2005; Grimm and Railsback, 2005). Here, we develop an IBM of *C. hyperboreus* encompassing observed individual variation, and couple it to an established ecosystem model; NORWECOM.E2E. In synthesizing existing *C. hyperboreus* observational and experimental knowledge within this model framework, we study the development and spatial distribution of a population advected through environmental gradients within the Nordic Seas. Moreover, we ask whether low abundances in the Norwegian Sea can be attributed to (i) expatriation from the Greenland Sea Gyre, (ii) unsuccessful recruitment due to mismatch between reproduction and the timing of the spring bloom, (iii) poor growth due to interspecific competition with the highly abundant *C. finmarchicus* or (iv) top-down population control by planktivore predation. The first three hypotheses imply that *C. hyperboreus* encounters unfavourable conditions when advected into the Norwegian Sea, in line with the established view of environmental control on this species' distribution. The latter (iv), however, implies that *C. hyperboreus* has the ability to thrive under Norwegian Sea environmental conditions, which is a new perspective that may call for a revision of the current understanding of this calanoid copepod.

2. Material and methods

2.1. NORWECOM.E2E

The NORWegian ECOlogical Model system End-To-End (NORWECOM.E2E) is a merger of an NPZD model for plankton and nutrient cycling (Aksnes et al., 1995; Skogen et al., 1995) and different IBMs developed initially for zooplankton (Hjøllo et al., 2012) and fish (Utne et al., 2012). The system also includes modules for ocean acidification (Skogen et al., 2014) and contaminants (Green et al., 2011), and NORWECOM.E2E couples all components into one, integrated ecosystem model where one can use all or a selected number of modules in a simulation.

In this study, we present a newly developed IBM for *C. hyperboreus* (Section 2.2), which is used together with the NPZD and an IBM module for the congener *C. finmarchicus*. Physical ocean fields (velocities, salinity, temperature, water level and sea ice) are taken from a hindcast simulation (Budgell, 2005; Lien et al., 2006) using the ROMS model (Shchepetkin and McWilliams, 2005). The horizontal grid in the model domain (Fig. 1) is identical to a subdomain of the original ROMS grid, with a spatial resolution close to 20 × 20 km.

The NPZD is coupled to the physical model through light, hydrography and the horizontal and vertical movement of water masses. Prognostic variables are dissolved inorganic nitrogen (DIN), phosphorous (PHO) and silicate (SI), two different types of phytoplankton (diatoms and flagellates), two detritus pools (N and P), diatom skeletal (biogenic silica) and oxygen. Two types of generic zooplankton (meso- and microzooplankton) are included in the NPZD based on a module taken from the ECOHAM4 model (Moll and Stegert, 2007; Stegert et al., 2009; Pätsch et al., 2009). Processes in the NPZD are primary and secondary production, grazing by zooplankton on phytoplankton, and detritus, respiration, algae death, remineralization of inorganic nutrients from dead organic matter, self shading, turbidity, sedimentation, resuspension, sedimental burial and denitrification. Remineralization takes place both in the water column and in the sediments. Particulate matter has a sinking speed relative to the water and may accumulate on the bottom if the bottom stress is below a certain threshold value, or become resuspended if the bottom stress is above a limit. Parameterization of the biochemical processes is taken from the literature based on experiments in laboratories and mesocosms, or deduced from field measurements (Aksnes et al., 1995; Pohlmann and Puls, 1994; Mayer,

1995; Gehlen et al., 1995; Lohse et al., 1995, 1996; Bode et al., 2004; Garber, 1984).

The incident irradiation used in the biochemical model is formulated based on Skartveit and Olseth (1986, 1987) using short wave radiation outputs from the ROMS simulation, and corrected linearly at the sea surface using the modelled ice concentration. Typical winter values of Atlantic Water in the Norwegian Sea has been used as nutrient initial fields (F. Rey, pers.comm.), together with some small initial amounts of phyto- and zooplankton. These values are also used at the open boundaries. Inorganic nitrogen is added to the system from the atmosphere, while there are no river inputs of nutrients. To absorb inconsistencies between the forced boundary conditions and the model results, a 7 gridcell "Flow Relaxation Scheme" (FRS) zone (Martinsen and Engedahl, 1987) is used around the open boundaries.

2.2. New Calanus hyperboreus IBM module

We here describe the *C. hyperboreus* IBM following the overview, design concepts and details (ODD) protocol (Grimm et al., 2006, 2010) to enhance readability and reproducibility of individual-based models.

2.2.1. Purpose

The *C. hyperboreus* IBM builds on an existing IBM for *C. finmarchicus*, but is adjusted to capture key traits of *C. hyperboreus* from the scientific literature. Our main purpose with this model is to study the spatial distribution and life history variation of *C. hyperboreus* in relation to the environment of the Nordic Seas. In addition, the model has been constructed so that estimates of annual biomass production and total food consumption can be investigated. Since the IBM is set up as a module in NORWECOM.E2E it can also be used to investigate interactions between the organisms included in this model system.

2.2.2. Entities, state variables and scales

Model entities comprise individual copepods, hereafter referred to as "compupods" for easier separation between modelled and actual organisms (following Maps et al., 2014), and their environment. Compupods are simulated through a full life cycle from eggs to spawning adults (13 stages, Table 1). Each compupod is associated with an attribute vector (Chambers, 1993; Huse et al., 2018) consisting of 17 states including the structural weight, fat reserves, horizontal and vertical position and age, as well as parent and (possible) death reason (Table 1). Due to the numerically vast numbers of *C. hyperboreus* in the Nordic Seas, each compupod is assumed to represent a varying number of identical siblings following the super-individual (SI) approach (Scheffer et al., 1995). In addition to the attribute vector, compupods also keep a strategy vector (Huse et al., 1999) onto which the behavioural strategy is coded. In the present model, the strategy vector contains three behavioural and life history traits or genes (Table 1) used to determine the vertical annual cycle: overwintering depth (OWD), wake up day from diapause (WUD) and daynumber for descending to diapause (enter diapause day, EDD). The WUD trait was first presented by Fiksen (2000), while OWD is from Huse et al. (2018) and EDD is introduced in the present work. The IBM is coupled to the surrounding environment through the physical forcing, the NPZD model and other IBMs in the NORWECOM.E2E model system (only *C. finmarchicus* IBM in the present study), and is flexible in the way that it operates on the same spatial grid as the physical model.

2.2.3. Process overview and scheduling

Processes governing the compupods are feeding, growth, movement, mortality and reproduction, and the IBM is run with a time step of one hour. The first four processes are updated by the hour, while reproduction is computed on a 24 h (daily) basis. Compupods start feeding at stage C3, and development up to this point is temperature dependent predicted by a Belehradek's function (Conover, 1967). From C3, growth is calculated as a function of food density, temperature and size using a functional response type 2 relationship (Carlotti and Wolf, 1998). Growth is accumulated in the structural weight, and also stored as fat for stages C4–C6. During times of negative growth, stored fat is depleted before the structural weight is reduced. Compupods are assumed to change stage when a stage specific critical weight is achieved (Table 2). Movement is both vertical, on diel and seasonal cycles, and horizontal in passive drift with ocean currents. A sex ratio of 1:1 is assumed and all males are killed when becoming adults. Female compupods spawn in batches, and the total number of eggs is a function of their fat reserves. Mortality consists of (i) unspecified causes through a stage dependent death rate, (ii) starvation when the weight goes below a critical weight, (iii) exhaustion if a maximum number of eggs have been spawned, (iv) size-dependent predation from pelagic, mesopelagic and tactile predators, and (v) extra mortality outside the Greenland and Iceland Seas (see Discussion). The total mortality rate is adjusted based on the total stock biomass, simulating density-dependent processes and as a way of tuning the model to better fit with stock biomass estimates of *C. hyperboreus* in the Nordic seas.

2.2.4. Design concepts

Emergence

Spatial and temporal population dynamics emerge from the growth and behaviour of individual compupods. At the individual level, compupod attributes like position and fat reserves emerge from interactions between individuals and the modelled environment.

Adaptation

The three genes in the strategy vector are inherited from mother to offspring and remain fixed over a compupod life cycle. However, the gene frequency at population level will to some extent be subject to adaptation through varying reproductive success among the compupods. Individuals with the "better" genes (e.g. in timing of descent and ascent) will produce more offspring and over time make a larger contribution to the total gene pool, thus improving the fitness of the population as a whole.

Sensing

Individuals are assumed to be able to sense the ambient chlorophyll and light levels, and to be aware of their own vertical position. Hence, they may locate the depth of chlorophyll maximum, avoid the upper layers during sunlight and reach the correct depth for overwintering (OWD). Compupods are also assumed to sense the day number, which is used for limiting spawning to (i) winter (November–March) and (ii) every 10th day (see Reproduction), and for deciding when to descend to and ascend from overwintering.

Interactions

The IBM for *C. hyperboreus* enforces grazing on phytoplankton and predation on microzooplankton in the NPZD in competition with the IBM for *C. finmarchicus*. Both IBMs are two-way coupled with the NPZD, meaning that the IBMs receive input on food density from the NPZD, and consumption in the IBMs is updated as reduced phyto- and microzooplankton availability in the NPZD. Feeding is modelled one individual at a time, and local food resources will be higher for those eating first. Hence, there is competition for food both for individuals from the same IBM, and between the two IBMs.

Stochasticity

Stochasticity is used at initiation with random distribution of the genes in the strategy vector as well as the initial position of compupods (though within defined limits, see Initialization below). Feeding order is computed at random each time step, both between the different IBMs and between all SI for a given IBM. There is also a random walk component in the horizontal movement of an SI to represent sub grid diffusion processes. When an SI reaches the adult stage, sex is decided by random and all males are killed. Nauplia N1 and N2 are given a random vertical position within the upper 40 m each time step.

Collectives

Modelled compupods are SI that each represent one or more identical siblings with similar attributes and strategies, but that die off one by one.

Table 1
The attribute and strategy vectors.

Attribute/Strategy	Explanation
Alive	Dead = 0, Alive = 1
Position	Gridposition (x,y,z)
Mynumb	Unique SI identifier
Inumb	Internal number
Stage	Egg, Nauplia N1–N6, Copepodite C1–C6
Age	Age in years
Sweight	Structural weight in μg C
Fat	Fat weight in μg C
Lstage	Stage longevity in days
Moult	Moult cycle fraction for egg and N1–C2
Maxegg	Number of eggs to be spawned
Cumegg	Accumulated number of eggs spawned
Activity	0 = diapause, 1 = active, 2 = descending 3 = ascending
Sex	0 = male, 1 = female
Death	Cause of death
Parent	SI identifier of parent
OWD	Overwintering depth (600–1000 m)
WUD	Wake-up-day from diapause (March 1 – May 15) (Hirche, 1997)
EDD	Enter-diapause-day (July 5 – August 25) (Hirche, 1997)

Table 2
Overview of model parameters.

Parameters	Value	Unit	Reference
N1 weight (W)	0.53	μg C	Jung-Madsen et al. (2013)
N2	0.41	μg C	Jung-Madsen et al. (2013)
N3	0.29	μg C	Jung-Madsen et al. (2013)
N4	1.20	μg C	Jung-Madsen et al. (2013)
N5	2.40	μg C	
N6	3.60	μg C	
C1	6	μg C	Hirche (1997)
C2	24	μg C	Hirche (1997)
C3 min W	82	μg C	Hirche (1997)
C3 critical W = C4 min W	418	μg C	Hirche (1997)
C4 critical W = C5 min W	1430	μg C	Hirche (1997)
C5 critical W = C6 min W	2024	μg C	Hirche (1997)
Stage dependent mortality (egg)	10	% d^{-1}	
Stage dependent mortality (N1–N5)	2.2	% d^{-1}	
Stage dependent mortality (N6–C2)	0.15	% d^{-1}	
Stage dependent mortality (C3–C6)	0.0	% d^{-1}	
Egg stage longevity parameter (Eq. (1))	1016		Jung-Madsen et al. (2013)
N1	904		Jung-Madsen et al. (2013)
N2	1555		Jung-Madsen et al. (2013)
N3	4449		Jung-Madsen et al. (2013)
N4	5245		Jung-Madsen et al. (2013)
N5	9042		Conover (1967)
N6	6510		Conover (1967)
C1	1446		Conover (1967)
C2	16 276		Conover (1967)
Maximum number of eggs	1500		Conover and Siferd (1993)
Minimum structural spawning weight	869	μg C	
Eggweight	0.76	μg C	Jung-Madsen et al. (2013)
Eggfat	0.55	μg C	Jung-Madsen et al. (2013)
Clutch size	150	eggs	Hirche and Niehoff (1996)
I_{max}	0.0266	$hour^{-1}$	Campbell et al. (2009)
Q_{10}	2.0		Campbell et al. (2009)
QR_{10}	1.211		
i_1 (Eq. (2))	100		Campbell et al. (2009)
r_1 (Eq. (3))	$4 \cdot 10^{-4}$		
r_2 (Eq. (3))	0.2		
a (Eqs. (2) and (3))	0.8		Campbell et al. (2009)
λ (Eq. (4))	0.2		
Diapause metabolism	0.1	% day^{-1}	Fiksen (2000)
VM1 (daydepth, C4–C6, Eq. (6))	13		Huse et al. (2018)
VM2 (daydepth, C4–C6, Eq. (6))	20 500		Huse et al. (2018)

Observation

For model analyses, all SI and their attributes are stored every 48 h, as well as daily fluxes between the different species and processes, e.g. biomass of phytoplankton eaten by *C. hyperboreus* and dead biomass of *C. hyperboreus* from starvation.

2.2.5. Initialization

Initial distribution fields simulate a *C. hyperboreus* population overwintering in the Greenland Sea basin. First, 50,000 SI are distributed randomly between 600 and 1000 m depth and between 70–78°N and 22°W-6°E, restricted to positions where the surface temperature is below 2.5 °C (Arctic water). The internal number in each SI are the same, and the number of SI are divided equally between copepodite

stage C3, C4, C5 and adult C6 with weights of 200, 800, 1800 and 2600 μg C, respectively, and a fat content of 61% for C4–C6 (mean fat content in copepodites C4–C6 in Scott et al., 2000). The three genes describing the seasonal vertical cycle (WUD, OWD and EDD) are given as random numbers within a fixed range taken from observational studies (see Table 1). Following, the model is run in 25 sequences using physical forcing from 1995, and the output from December 30 on the final run is stored and used as the initial distribution field for the *C. hyperboreus* population of the present study. Our main simulation starts on January 1, 1995, and the biology is allowed to evolve over 26 years where the first 16 will be referred to as "spin-ups" and the latter 10 as the "basic simulation" years. Forcing from 1995 was chosen since this is the first year with available forcing, and is used throughout to have control over the environmental conditions when evaluating model performance.

2.2.6. Input data

Input data on light, wind, currents, temperature, salinity and ice are taken from a previously validated simulation of the ROMS model (Shchepetkin and McWilliams, 2005; Budgell, 2005; Lien et al., 2006), while food availability comes from the NPZD of NORWECOM.E2E (see Section 2.1). The IBM is, however, strictly not driven by the NPZD considering that these are fully (two-way) coupled.

2.2.7. Submodels

Feeding and growth

Compupods start feeding at stage C3, and mean development time up to this point (egg–C2) is only temperature dependent and predicted by a Belehradek's function (Conover, 1967; Jung-Madsen et al., 2013):

$$D = a \cdot (T + 12.7)^{-2.05} \tag{1}$$

where a is a stage dependent parameter and T is the temperature in °C.

Stages C3–C6 are considered omnivorous and feed on a combination of phytoplankton (two types; flagellates and diatoms) and microzooplankton from the NPZD. The scientific literature is not consistent with regards to the relative importance of grazing *versus* predation on microzooplankton in *C. hyperboreus*' diet (e.g. Søreide et al., 2008; Campbell et al., 2009), so for simplicity and in compliance with the *C. finmarchicus* IBM we set feeding as non-selective reflecting the relative proportion of each food source in the environment. Total ingestion is calculated with a functional response type 2 relationship as a function of food density ($food$), T and size (W) (Carlotti and Wolf, 1998):

$$I = I_{max} \cdot {Q_{10}}^{T/10} \cdot W^{a} \cdot \frac{max(0, food - thres)}{i_1 + max(0, food - thres)} \tag{2}$$

This relationship has been parametrized based on observational data from Campbell et al. (2009) (Table 2). To avoid the phyto- and microzooplankton fields from becoming locally extinct, minimum concentration thresholds ($thres$) set to 0.1 mg N m^{-3} for each food source is not available for grazing. This is a purely technical solution and not based on an observation that calanoids are unable to utilize all available resources in the environment, so we compensate for this by supplying an extra food source with a constant concentration of 0.3 mg N m^{-3} available for consumption by the compupods. Note that this "background food" is low compared to the other three resources which together may reach concentrations > 200 mg N m^{-3} during a growth season.

Respiration consists of basic and active metabolism. The basic part is a function of compupod size and ambient temperature, and the active part is a constant fraction (20%) of the ingestion I:

$$R = r_1 \cdot W^{a} \cdot {QR_{10}}^{T/10} + r_2 \cdot I \tag{3}$$

where r_1, r_2 and QR_{10} are constants calculated from observations (Table 2). Egestion is a constant proportion of the ingestion:

$$E = \lambda \cdot I \tag{4}$$

and growth emerges as the sum of the ingestion minus respiration and egestion:

$$G = I - R - E \tag{5}$$

Positive growth is added only as structural weight for stage C3, since we were not able to find data on % fat content in C3 for *C. hyperboreus*. For C4–C6 growth is first added as fat reserves up to 61% of total weight (Falk-Petersen et al., 2000; Scott et al., 2000), and thereafter added in a 39:61 ratio between structural weight and fat. In periods of negative growth, fat reserves are depleted before the structural weight is affected. As in the *C. finmarchicus* IBM, compupods are assumed to change stage when a stage specific critical weight is achieved (Table 2) at a moulting cost of 10% of the structural weight (same as *C. finmarchicus* IBM). Individual variability in the size at stage will be within the ranges of the stage specific critical weights (see Table 2). When in diapause, compupods do not feed and a resting metabolism of 0.1% d^{-1} is assumed similar to the *C. finmarchicus* IBM based on Fiksen (2000).

Reproduction

Spawning is modelled as a capital breeding strategy (i.e. fuelled by energy surplus stored from the previous season), and takes place in winter between November 1 and April 1 when *C. hyperboreus* are in the deep (Hirche and Niehoff, 1996; Gislason, 2018). To commence spawning, the female compupod must have attained a structural weight > 869 μg C (= C6 minimum weight + 10%), and enough fat reserves to spawn a minimum of one clutch of eggs. The total number of eggs a compupod may produce is given by its fat weight divided by the egg weight (Table 2). If the criteria for initiating spawning are fulfilled, a new offspring SI is produced. As *C. hyperboreus* are batch spawners and to avoid a very high number of small SI, eggs are subsequently spawned in clutches of up to 150 eggs every 10th day (Hirche and Niehoff, 1996; Hirche, 2013), and each events generates one new SI. The $inumb$ (number of identical siblings represented by the super-individual) of the new SI is given by the clutch size multiplied by the parent $inumb$. Following reproduction, the fat reserves of the parent SI is reduced by an amount corresponding to the clutch size multiplied by the egg weight.

Movement

Horizontal movement simulates passive drift with the ocean currents, and is computed using the velocity fields from the ROMS model and a 4th order Runge–Kutta method. In addition, we include a random component representing sub-grid diffusion processes.

Vertical movement simulates diel and seasonal migrations by which compupods change their depth position (Z). For non-diapausing compupods, the vertical positioning is stage dependent. Eggs and nauplii are positively buoyant and after release (at depth) they will ascend towards the surface with a speed of 6 m d^{-1} (Jung-Madsen et al., 2013) until they reach 20 m depth. After that, nauplii and compupods stages C1–C3 remain at the depth of the maximum chlorophyll (Daase et al., 2008). Larger compupods (C4–C6) undertake diel vertical migrations (DVM) where the day depth (DD) is calculated as a function of individual size (Ohman and Romagnan, 2016):

$$DD = VM_1 + L \cdot VM_2 \tag{6}$$

Based on this formulation, the daytime depth for C4, C5 and C6 is around 70, 95 and 105 m respectively. At night, active C4–C6 stay at the depth of chlorophyll maximum.

Controlling factors for the initiation and termination of diapause in calanoid copepods is to date poorly understood, but hypothesized to be related to internal state (Johnson et al., 2008), predator avoidance (Kaartvedt, 2000) or a combination of internal/external factors and gene expression (Häfker et al., 2018). In our model, ascent from and descent to diapause is determined by the WUD and EDD genes (Table 1), which can be viewed as a simplification of the results by Häfker et al. (2018). The genes are static in the sense that they do not include any direct information on the condition of the compupods, but there is an indirect link to the environment as the time used in

diapause and the time available for feeding will have an impact on the available fat reserves and therefore on the contribution from a given SI to the next generation. Compupods may enter diapause from stage C3, and during diapause they reside at the overwintering depth (OWD) given by the strategy vector. During ascent and descent the compupods move at a speed of 2 m hour^{-1}.

Mortality

Young developmental stages (egg–C2) suffer instantaneous mortality rates which decline as the compupod develops (Table 2). For older stages, mortality is assumed to be primarily driven by visual and tactile predation, starvation and spawning stress.

Visual predation from pelagic and mesopelagic fish is (for stages C1–C6) estimated as a function of ambient light, predator visual capability and compupod size, with equations and parameters similar to the *C. finmarchicus* IBM described in Huse et al. (2018). The total rate is further linearly modified by temperature $pred = pred \cdot \max(0., T - 2.5)$, so that visual predation is an increasing function of T and zero at 2.5 °C. This adjustment is based on key pelagic and mesopelagic fish distributions in relation to temperature in the Nordic Seas (Dale et al., 1999; Misund et al., 1998; Olafsdottir et al., 2019). Tactile predation is also set up as in the *C. finmarchicus* IBM as a function of predator density, search area and swimming velocity (Huse et al., 2018), in the current study also linearly modified by temperature the same way as visual predation. Visual and tactile predator densities are taken from Skjoldal (2004).

Starvation is implemented as additional mortality of 0.6% d^{-1} when the structural weight gets below 40% of the stage specific moulting weight. This means that compupods will suffer starvation mortality around the time when all fat is lost, since the total weight (structural weight + fat) determines when a compupod will moult into the next stage and the structural weight to fat ratio is kept at 39:61.

Compupods advected outside the Greenland and Iceland Seas will suffer additional mortality of 1% d^{-1}, based on the low abundances observed from these areas (Broms et al., 2009; Strand et al., 2020) (see Discussion). Given the wide range and uncertainty of mortality, the total rate is treated as a variable to better fit with the estimated *C. hyperboreus* overwintering biomass from Visser et al. (2017). On January 1 every year, a correction factor, C_{mort}, is calculated and multiplied with mortality rates the following year, simulating density dependent mortality processes. The factor follows a log-like function:

$$C_{mort} = (0.0738 + 0.5 \cdot (1 + \frac{1}{B} \cdot \ln \frac{A}{1 - A})) \cdot (C_{max} - C_{min}) + C_{min} \quad (7)$$

where $C_{max} = 1.4$ and $C_{min} = 0.6$, $B = 4.59$ and A is a function of the biomass on January 1 and the assumed long term mean biomass of *C. hyperboreus* set to 3 million tonnes of carbon (based on Visser et al. (2017)), so that $C_{mort} = C_{max}$ when the actual biomass is 6 MT, and $C_{mort} = C_{min}$ when the biomass drops to 1.5 MT.

Mortality is implemented as a reduction in the internal number of the compupod until *inumb* goes below 1 and the SI is taken out of the population. Super-individuals who become males at C6, spawn the maximum number of eggs, spend more than two years in the same stage or are advected out of the model domain are taken out directly irrespective of *inumb*.

2.3. Calanus finmarchicus IBM

The *C. finmarchicus* IBM has been documented in line with the ODD protocol in Huse et al. (2018). Our purpose of including this module in the current study is to account for indirect competition for food considering that *C. finmarchicus* is the dominant grazer in the Norwegian Sea ecosystem (Broms et al., 2009; Strand et al., 2020). Briefly, the design and processes included in the *C. finmarchicus* module are as for *C. hyperboreus*, but with parameter settings as described in Huse et al. (2018) and Hjøllo et al. (2021). The main differences are: (i) *C. finmarchicus* compupods cannot enter diapause before stage C5, and decisions regarding overwintering is driven by a start date to allocate fat (AFD) and a relative fat content to be obtained before descending, (ii) feeding starts at N3 and fat is not accumulated before stage C5, (iii) mortality rates in autumn for non-overwintering *C. finmarchicus* compupods is slightly enhanced to better fit with stock biomass estimates of *C. finmarchicus* in the Nordic Seas, (iv) *C. finmarchicus* is modelled as an income breeder (spawning is fuelled by the spring bloom) and (v) initial distributions for the *C. finmarchicus* IBM is taken from Hjøllo et al. (2012). The two-way coupled NPZD and *C. finmarchicus* IBM have been evaluated by comparison with field data from the North Sea, Nordic Seas and the Barents Sea (Skogen et al., 2007; Hjøllo et al., 2012; Skaret et al., 2014; Hjøllo et al., 2021; Gao et al., 2021).

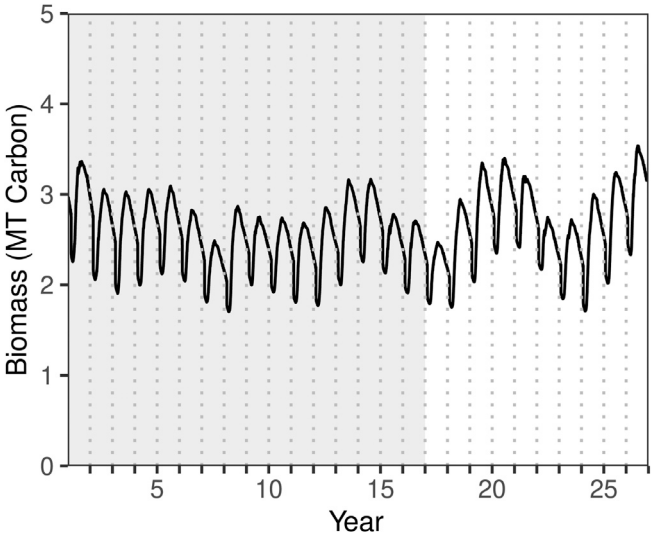

Fig. 2. Modelled *C. hyperboreus* biomass for the total simulation of 26 years (main simulation, Table 3) using forcing from 1995 (grey: 16 years spin-up period, white: basic simulation). Dotted, vertical lines indicate January 1 each year.

3. Results

3.1. Temporal and spatial population dynamics

Modelled *C. hyperboreus* population biomass is relatively stable over the 16 years spin-up plus 10 basic simulation years (Fig. 2), with a mean C_{mort} (Eq. (7)) of 0.96 and without any trend (slope = -3×10^{-4} year^{-1}). Over a growth season, the population increases in biomass by around 50% from a mean minimum of 2 MT carbon in early April to a mean maximum at 2.9 MT carbon in late August. We do observe a periodicity in the interannual biomass fluctuations of 3–4 years, which seems to be driven by the total biomass of C4 (Fig. 3) and may relate to the median life-cycle length at population level (see Individual growth and life histories below). It may also to some degree be an artefact of the model arising from the use of C_{mort} to fine-tune the total mortality rates, whereby the population alternates between periods of good and weakened recruitment.

Stage C4 compupods constitute the largest biomass in the population, followed by C5 and C6 (Fig. 3). Averaging over the basic simulation years, the C4 biomass (1.12 MT carbon) is close to the sum of C5 (0.65 MT carbon) and C6 (0.60 MT carbon). This is due to the higher modelled abundance of the smaller C4 compupods (Fig. 3 lower left panel), which is more than twice the sum of C5 and C6. Stage C6 has the largest fluctuation in mean individual body mass, due to the seasonal *loss* of fat from spawning.

Biomass aggregates spatially in the Greenland Sea, though there is also a fairly large pool in the Iceland Sea (Fig. 4, left panel). Of the total biomass, about 51% of the stock is found in the Greenland Sea, 30% in the Iceland Sea and 17% in the Norwegian Sea. Except for the

Table 3
Overview of simulations, all run with physical forcing from year 1995.

Simulation	Purpose	Description
(1)	Create initial population field	50,000 super-individuals initiated between 600–1000 m depth, 70–78°N and 22°W-6°E, restricted to positions where the surface temperature is below 2.5 °C. Population allowed to evolve over 25 years.
(2)	Main simulation	End population from (1) used as start field. 16 years "spin-up" and 10 "basic simulation" years.
(3)	No geographically defined mortality	Same as (2), but without added 1% d^{-1} mortality for compupods advected into the Norwegian Sea.

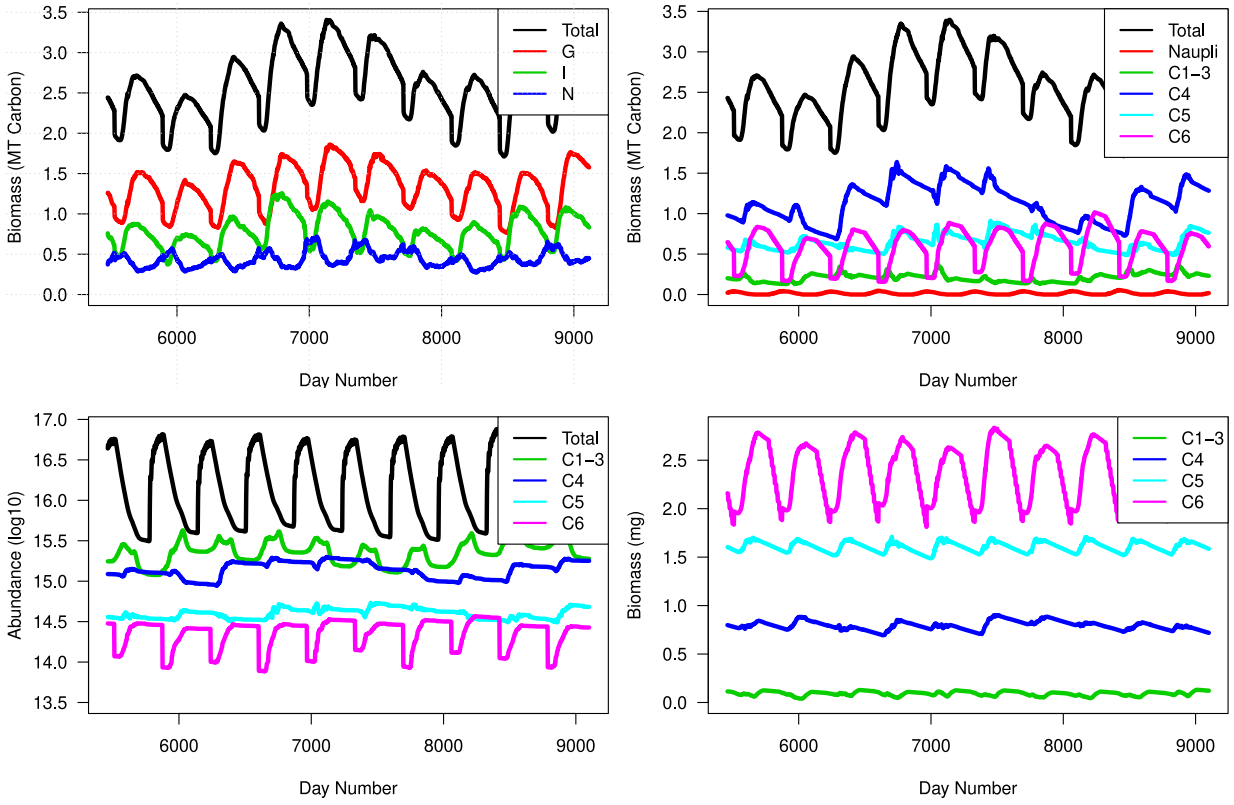

Fig. 3. Biomass and abundance of *C. hyperboreus* over the basic simulation (year 16–25). Upper left: Biomass divided into areas: Total, Greenland Sea (G), Iceland Sea (I) and Norwegian Sea (N). Upper right: Modelled biomass by stage. Lower left: Abundance (log10) by stage. Lower right: Mean individual biomass by stage.

annual cycle, the biomass is relatively stable in all these regions (Fig. 3). In a separate model run excluding the additional 1% d^{-1} mortality for compupods outside the Greenland and Iceland Seas (simulation 3, Table 3), the population in the Norwegian Sea outperforms the other regions and gradually takes over as the dominant stock fraction (Fig. 4, right panel). The main simulation lays the basis for results displayed in the rest of the Results section unless stated otherwise, but we will revisit simulation 3 in the Discussion.

The seasonal biomass development of *C. hyperboreus* compupods differs between the three regions (Fig. 5A). Biomass in the upper 200 m of the Norwegian Sea peaks in May–June, while in the Greenland and Iceland Seas it peaks in June–July. Compupod biomass peaks and differences in timing between the three regions seem to be linked to the seasonal food availability in the model environment (Fig. 5C).

3.2. Individual growth and life histories

The full life cycle of an arbitrary SI is shown in Fig. 6A. This compupod reaches stage C3 in about 7 months and C4 after 17 months, which is close to the median development times at population level (Table 4). It becomes C5 after 40 months, which is longer than the median time in the population, and it requires two growth seasons to become both C5 and C6. The total life cycle is six years, and overwintering stages are C3, C4 (twice), C5 (twice) and C6. The structural weight drops slightly during first diapause since fat is not accumulated before stage C4. During subsequent diapauses, the overwintering metabolism causes a drop in the fat reserves but not the structural weight (red and black lines Fig. 6A). In the final diapause the compupod spawns, seen as a major drop in fat and a simultaneous peak in egg production, and it dies of exhaustion after producing the maximum number of eggs (1500).

At population level, 73% of the SI reach C5 before the 3rd winter, and average time to maturity (egg to C6) is 3.2 years. The fastest growing SI reaches C5 in only 149 days. Nevertheless, few compupods have short life cycles of 1–2 years, while 3–5 years length prevails in the population (Fig. 7). Growth is temperature and food dependent, and spatial variation in environmental conditions gives individual variation in the model population. The shortest life cycles correspond to more time spent within the Iceland and Norwegian Seas, while longer life cycles (> 3 years) are characteristic for compupods that have spent more time in the Greenland Sea (Fig. 6).

A majority of the compupods (95%) manage to reach the first overwintering stage (C3) in time for overwintering, which is often considered critical for copepod survival in nature. A considerable amount in the modelled population (12%) also reach stage C4 before first diapause.

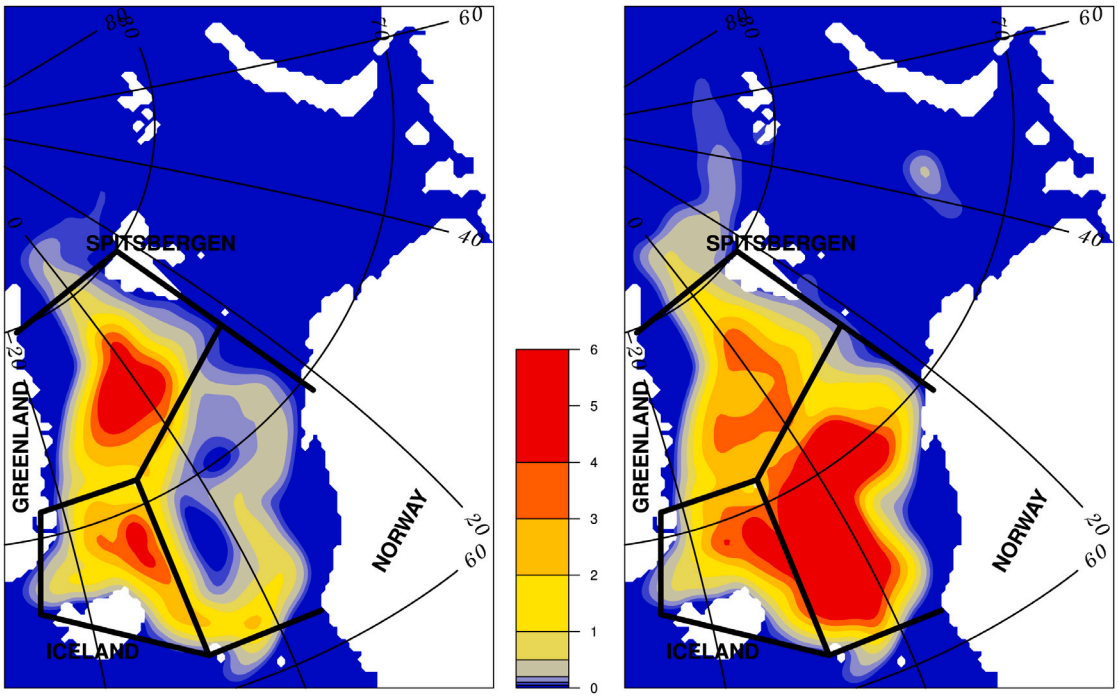

Fig. 4. Annual mean depth integrated (g C m^{-2}) *C. hyperboreus* biomass for basic simulation years 16–25. Black lines delineate the regions defined as the Greenland Sea (northernmost region), Iceland Sea (south west) and Norwegian Sea (south east), and the two panels display biomass distribution with and without geographically defined mortality rates (simulations 2 and 3 from Table 3). Left panel: 1% additional mortality d^{-1} for compupods in the Norwegian Sea. Right panel: no added mortality in the Norwegian Sea.

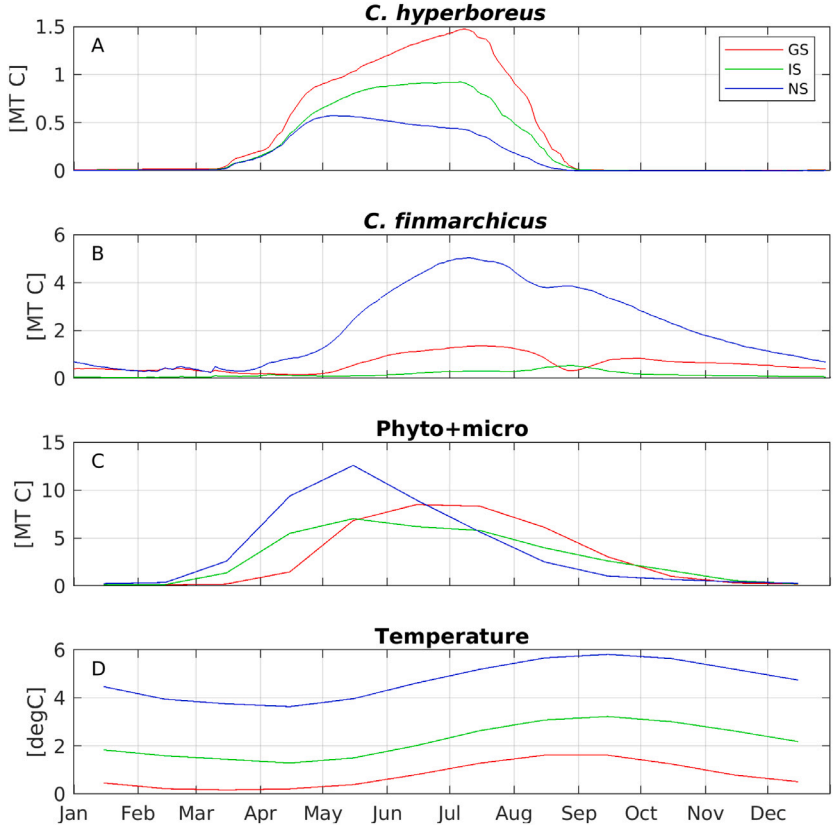

Fig. 5. Region-specific seasonal development of (A) *C. hyperboreus* and (B) *C. finmarchicus* biomass (both top 200 m), (C) phyto- and microzooplankton biomass (top 200 m) and (D) temperature (average of top 200 m), averaged over the basic simulation years.

Table 4
Summary of key model outputs on compupod development time (number of days to reach a given stage) and area-specific retention time (number of days from hatching of eggs) over the basic simulation, changes in compupod strategies (strategy vector) from initialization to the end population, relative distribution of population biomass and egg production in the three areas (GS: Greenland Sea, IS: Iceland Sea, NS: Norwegian Sea), and area-specific mortality causes (% of dead biomass) in an average year.

Development time (days to reach)	**Stage**	**Mean**	**Median**	**SD**
	C3	212	191	87
	C4	540	512	191
	C5	934	893	217
	C6	1173	1205	275
	Area			
Retention time (days from hatching)	GS	211	74	356
	IS	88	54	116
	NS	262	88	383
		OWD	**EDD**	**WUD**
Strategies	Initial (mean)	800 m	July 31	April 06
	End (mean)	823 m	July 28	March 26
		GS	**IS**	**NS**
Relative distribution	Biomass (%)	51	30	17
	Egg production (%)	56	28	15
Mortality causes (%)	Pelagic predation	3	9	16
	Mesopelagic predation	2	6	9
	Tactile predation	1	7	10
	Outside GS	0	3	45
	Spawning exhaustion	23	17	5
	Insufficient development	10	8	1
	Male sex	60	51	14
	Starvation	0	0	0

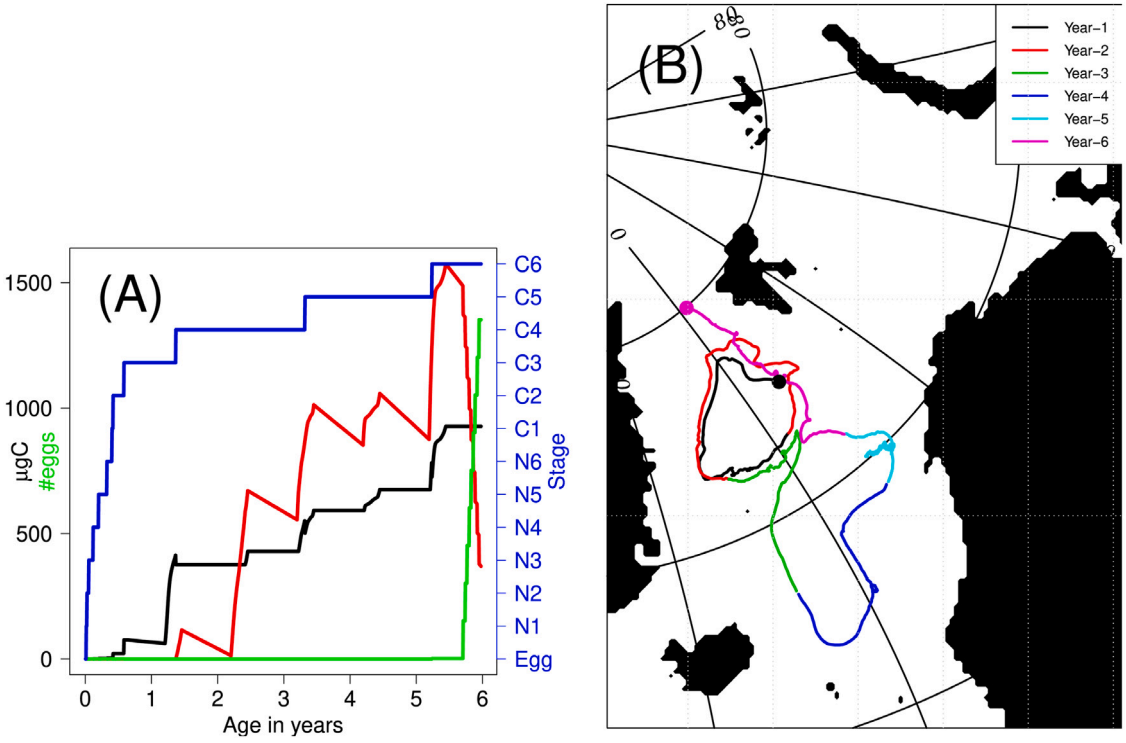

Fig. 6. (A) Life cycle showing structural weight (µg C, black line), fat (µg C, red line), cumulative egg production (green line) and stage number (blue line) for an arbitrary compupod. (B) Corresponding horizontal position for the same SI over the 6 years life cycle, where the black dot corresponds to the start and pink dot to the end position of the super individual.

3.3. Advection

The model demonstrates how *C. hyperboreus* is following the main circulation patterns with a counterclockwise transport in the Nordic Seas, enabling individuals to return to the core area in the Greenland Sea after being recirculated there. The compupod in Fig. 6 spends the first 2.5 years of its life circulating in the Greenland Sea Gyre, before it is transported south towards the Iceland Sea (year 3), northwards into the Norwegian Sea (year 4–5) and back into the Greenland Sea and Fram Strait (Year 6) (Fig. 6B).

The model also suggests a small transport of compupods into the Arctic through the Fram Strait, and an even smaller transport southwards into the North Sea (mean 800 T carbon per year over the basic simulation). With a mean population biomass of 3 MT carbon, 13% of the stock (0.4 MT C) is advected out of the model area each year.

Retention time of compupods within the GS, IS and NS increases with the size of the respective areas in Fig. 4. Median retention times

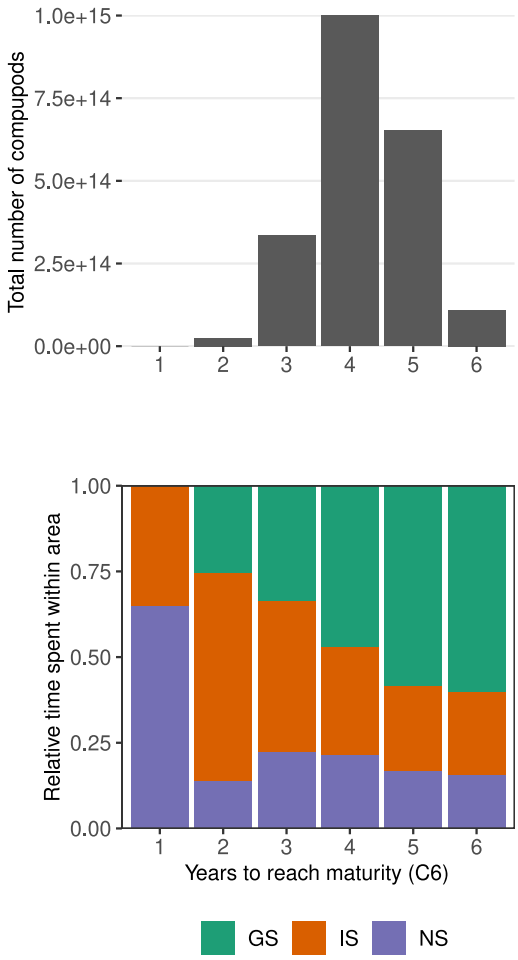

Fig. 7. Distribution of life cycle length in the modelled *C. hyperboreus* population (top), and relative time spent within each of the model regions for compupod with the corresponding life cycles (bottom). Panels share x-axes. GS: Greenland Sea, IS: Iceland Sea, NS: Norwegian Sea.

in days from hatching ranges from 54 days in the Iceland Sea to 74 days in the Greenland Sea and 88 days in the Norwegian Sea (Table 4). Since most compupods require a minimum of three years to reach maturity (Fig. 7), this means that the majority will not remain within the area where they were hatched throughout the life cycle, but rather circulate between the three regions or leave the Nordic Seas altogether.

3.4. Reproduction

Annual egg production is about 3×10^{17} (roughly averaged to 950 eggs per female), and resembles the spatial population distribution in relative biomass. Yet, the Greenland Sea egg production is slightly higher (56% of the total compared to 51% for biomass), and the Iceland and Norwegian Seas slightly less than their respective biomass fractions. Since the relative biomass distribution between stages is similar in the three regions (results not shown) and egg mortality rates are the same across the model domain, this indicates that females in the Greenland Sea build more fat for spawning than those in the other regions. Most females complete spawning within one season, and less than 1% spawn during successive years. However, 25% of the females die before producing the maximum of 1500 eggs.

3.5. Trophic interactions

The modelled *C. hyperboreus* stock consumes on average 5 MT carbon each year, out of which 80% is phytoplankton. With a long term mean modelled biomass of 3 MT carbon, this gives a P/B-ratio of ~1.7. Starvation is a negligible mortality cause across the whole model domain (Table 4). Annual net growth is estimated to 3.1 MT carbon and should in a stable system balance the loss (mortality) terms. Visual, pelagic predation is close to the sum of mesopelagic and tactile predation in all areas, but mortality causes differs between the three regions in relative terms (Table 4). Death of males and spawning exhaustion are the main causes in the Greenland and Iceland Seas, while in the Norwegian Sea predation and the 1% extra rates specific for this area dominate the total mortality. Insufficient development (i.e. spending more than two years in the same stage) affects compupod mortality in both the Greenland and Iceland Seas, but is negligible in the Norwegian Sea.

Modelled biomass of *C. finmarchicus* in the Norwegian Sea is more than 3× the biomass of *C. hyperboreus* in the same area (Fig. 5). The two species ascend to the surface around the same time (~day 100), but peak biomass in *C. hyperboreus* occurs around two months earlier than for *C. finmarchicus*. This can be ascribed to differences in spawning strategies (capital breeding for the *C. hyperboreus* IBM and income breeding for the *C. finmarchicus* IBM), and also to higher mortality rates for active (i.e. non-diapausing) *C. hyperboreus* compupods. At the other side of the growth season, *C. hyperboreus* leaves the upper 200 m at a fixed date (mean late July, Table 4) while *C. finmarchicus* has a more prolonged descent period which gives a considerable biomass in the Norwegian Sea also beyond the summer (Fig. 5). It should be noted that in the simulation without 1% additional mortality for *C. hyperboreus* in the Norwegian Sea (Fig. 4 right panel), the biomass of *C. hyperboreus* in the Norwegian Sea increases dramatically even though there is competition for food between the two IBMs. So interspecific resource competition does not by itself seem to prevent a population of *C. hyperboreus* establishing here.

4. Discussion

Physics are commonly a missing link in zooplankton observational studies. Ideally, one should have complete knowledge of a zooplankters advective history to fully assess e.g. relationships between species distributions and environmental conditions. Modelling approaches that couple biological processes to the physical ocean environment are important for filling knowledge-gaps where observational studies fall short. The NORWECOM.E2E model system is a useful tool in this regard, and the individual-based model of *C. hyperboreus* enables us to gain new insight and also point at unresolved questions and inconsistencies regarding the current understanding of this species in its environment.

Development of compupods in our model fits well with existing knowledge of *C. hyperboreus* from observational studies. Hirche (1997) proposed 3–4 years as the most common life cycle length for *C. hyperboreus* in the Greenland Sea, while other studies have suggested shorter life cycles under more favourable environmental conditions (Diel, 1991; Gislason, 2018). In our simulations, a large portion of the population requires at least 3 years to develop from eggs to adults and the majority have life cycles of 3–5 years. Compupods with shorter life cycles (1–2 years) share the common feature that larger parts of the life has been spent in the Iceland and Norwegian Seas, where environmental conditions are more favourable in terms of food availability and temperature.

Long life cycles of 5–6 years were characteristic for compupods that had spent a greater part of their life in the Greenland Sea, and means that a compupod will overwinter in the same copepodite stage during successive winters. We cannot rule out the possibility that this is an artefact of the model dependent on the parameterization of respiration

rates or mortality from starvation creating unrealistically high survival rates for these compupods. Falk-Petersen et al. (2009) refers to personal communication with Hirche in suggesting that the life span of *C. hyperboreus* may be longer than 5 years, which also implies multiple overwintering phases in the same stage given that it must reach C3 to undertake diapause. Only 5% of our compupods needed 6 years to complete a life cycle, but 31% required 5 years to reach maturity (Fig. 7). Multiple diapauses in stage C6 seems realistic based on the experiments by Plourde et al. (2003), but we have not been able to find studies assessing whether this is possible also for stages C3–C5. This outcome of the model does however imply that the resource availability (phytoplankton and microzooplankton) in at least part of the Nordic Seas is limiting for *C. hyperboreus* development. Microzooplankton and phytoplankton have both been suggested as core in *C. hyperboreus*' diet measured from *in situ* observations (Søreide et al., 2008; Campbell et al., 2009). Ice algae might have been a missing resource component in our model system, though, a food source believed to be critical for the congener *C. glacialis* (Søreide et al., 2010). To our knowledge it is uncertain whether *C. hyperboreus* is able to utilize ice algae or not. Nevertheless, implementing an ice algae module in NORWECOM.E2E will be an important addition to the future development of this model system.

Biomass in our model population varies spatially between 0.2–8.5 g dry weight m^{-2} (assuming 60% carbon content of total dry weight), which is in the range of biomass observed from the Greenland (Hirche, 1991, 1997; Møller et al., 2006) and Iceland Seas (Astthorsson and Gislason, 2003). Advective transport circumvent the Norwegian Sea basins, which are almost devoid of *C. hyperboreus* biomass when additional mortality rates are implemented for this region (Fig. 2). A gradient of low (0.7 g dw m^{-2}) biomass northwards from the Lofoten Basin (69°N) with increasing biomass eastwards towards the Greenland Sea resembles the observations by Carstensen et al. (2012) from the West Spitsbergen Current. Compupod stage C4 dominates in our model population and has been reported as the most abundant stage also from observations (Hirche, 1997).

For planktonic organisms whose horizontal distribution is at the mercy of ocean currents, the presence of retention areas is of paramount importance for a stable population to exist. Within the Nordic Seas, three such retention areas exist in the form of cyclonic gyres: the Norwegian Basin and Lofoten Basin Gyres in the southern and northern Norwegian Sea, respectively, and the Greenland Sea Gyre in the central Greenland Sea. The latter is considered the main overwintering and retention area for *C. hyperboreus*. Our simulation without the 1% daily mortality increase for compupods transported outside of the Iceland and Greenland Seas indicates that *C. hyperboreus* could in fact establish a large and thriving population within the Norwegian Sea, and the gradient comparable to Carstensen et al. (2012) is reversed (Fig. 4, right panel). Hence we do not find expatriation from the Greenland Sea Gyre to be a likely explanation for the low abundances observed *in situ* in the Norwegian Sea. On the contrary, our simulations show that a large portion of compupods will visit more than one of our three regions in the Nordic Seas throughout a life time, due to the low median retention times (< 1 year) for each region and the species' multi-year life cycle. Thus, the whole Nordic Sea area can be regarded as a super-retention area for *C. hyperboreus*. We cannot rule out that the Greenland Sea receives *C. hyperboreus* e.g. from the Arctic Ocean, a potential source population not considered in our study. Nevertheless, other modelling studies raise doubt on whether it manages to complete a life cycle there (Ji et al., 2012; Kvile et al., 2018). A natural question thus arises as to why we need additional mortality in the Norwegian Sea to prevent a large population establishing there in the model, when observations show that *C. finmarchicus* is the dominant copepod within the Norwegian Sea (although *C. hyperboreus* is commonly found in smaller numbers).

The Greenland Sea gyre and the Norwegian Sea gyres differ significantly in terms of water mass origin. While the Norwegian Sea gyres are heavily influenced from inflow of warm saline water from the Norwegian Atlantic Current, the Greenland Sea Gyre is composed mainly of cold water transported by the East Greenland Current emanating from the Arctic Ocean. One possible explanation of low abundances in the Norwegian Sea could be that *C. hyperboreus*, when transported here, falls outside its preferred temperature regime. Strand et al. (2020) showed that *C. hyperboreus* is seldom found in surface water of Atlantic origin with temperature higher than 5 °C, and that peak densities are in Arctic water masses with temperatures lower than 2 °C. However, in developing this model we have not been able to find evidence in the existing literature that growth or reproduction of *C. hyperboreus* should be impeded under the temperature regime of the Norwegian Sea (Fig. 5). Rather, Henriksen et al. (2012) showed that temperature (0–10 °C) had no effect on egg or fecal pellet production of *C. hyperboreus* reared in laboratory. Food availability had a positive effect on *C. hyperboreus* fecal pellet production and growth in Henriksen et al. (2012), and is in our model system greater in the Norwegian Sea both in terms of total amount and length of the growth season. Mis-match between the timing of reproduction and the spring-bloom has also been proposed as an explanation for the low abundance of *C. hyperboreus* in the Norwegian Sea (Broms et al., 2009). In our simulations, the biomass peak in *C. hyperboreus* occurs earlier in the season and more tightly linked to the peak resource abundance in the Norwegian Sea compared to *C. finmarchicus*. Temperature-dependent development up to C3 is a potential weakness in our model in preventing resource dependent starvation rates for nauplii and young copepodite stages. However, the seasonal growth of resources start over a month later in the Greenland Sea compared to the Norwegian Sea (Fig. 5D). We therefore find mis-match between reproduction and food availability an unlikely explanation for the low abundances of *C. hyperboreus* in the Norwegian Sea given that the core population resides in the Greenland Sea.

Sainmont et al. (2014) argue, based on a theoretical model, that copepod species adapted to a short and intense foraging season would benefit from being capital breeders, while as the foraging season gets longer, being smaller and switching to income breeding becomes more advantageous. This fits well with observed differences in relation to spawning strategies and body size, as *C. hyperboreus* is a large capital breeder and *C. finmarchicus* is a smaller income breeder (Conover, 1988; Falk-Petersen et al., 2009). But in our simulations without added mortality, we find no evidence that *C. finmarchicus* outcompetes *C. hyperboreus* even though both species forage on the same resources. The *C. finmarchicus* IBM has a P/B ratio of 4.3 (Hjøllo et al., 2012) while for the *C. hyperboreus* IBM we have a P/B ratio of 1.7, and since *C. finmarchicus* is the most abundant and with highest turnover it should also be considered the major grazer in the Norwegian Sea model region. Nevertheless, the biomass of *C. hyperboreus* increases quite substantially in the Norwegian Sea without the added mortality, despite resource competition. Excluding the *C. finmarchicus* IBM from our main simulation altogether (not shown) increases the total mean biomass of *C. hyperboreus* by 0.5 MT C (~17%), so there is resource competition between the two IBMs. Nevertheless, food availability does not seem to be a major limiting factor for *C. hyperboreus* in the Norwegian Sea model region, and low total resource demand from the *C. hyperboreus* stock may be the reason for little competition between the two *Calanus* IBMs. Annual net primary production in the Nordic Seas have been estimated at 70–80 g C m^{-2} (Rey, 2004; Richardson et al., 2005) which is comparable to the production in NORWECOM.E2E (Skogen et al., 2018). The modelled *C. hyperboreus* stock consumes on average 2.6 g C d^{-2} y^{-1} in the Nordic Sea regions (main simulation), which amounts to grazing down 3%–4% of the annual production here.

Predation is the second largest mortality cause in the Norwegian Sea in our simulations, next to the 1% added mortality. In their model, Sainmont et al. (2014) assumes that copepod mortality is an allometric function of weight and the negative exponent ($^{-1/4}$) implies that larger individuals experience less predation. However, as Sainmont et al.

(2014) also point out, it can be argued that copepod mortality does in fact increase with increasing body size, particularity when exposed to visual predators (Aksnes and Utne, 1997; Eiane et al., 2002). Assuming parameters such as prey body contrast and shape being equal, Aksnes and Utne (1997) shows that the detection distance of a visually foraging fish on prey in the size range 1–4 mm increases more or less linearly, and that the slope of the linear relationship increases with increasing ambient light. With adult *C. hyperboreus* being more than twice as large (prosome length) as *C. finmarchicus* (McLaren et al., 1988), one would expect a considerably higher predation risk for *C. hyperboreus*, with increasing differences with decreasing depth during daytime.

This brings forward another important difference between the Norwegian and Greenland Seas; the amount of visually foraging planktivorous fish present. While the Norwegian Sea is well known for large stocks of pelagic zooplanktivores such as mackerel, herring and blue whiting (Utne et al., 2012), the Greenland Sea has little pelagic fish when measured as acoustic backscatter (Dale et al., 1999). Furthermore, Klevjer et al. (2020), found that the amount of mesopelagic fish steadily declined moving from the southern Norwegian Sea northeastward into the Iceland Sea. Also, Gjøsæter and Kawaguchi (1980) reports significantly lower biomasses of mesopelagic fish in the Greenland Sea (0.1 g m^{-2}) compared to the southern Norwegian Sea (2 g m^{-2}). Dalpadado et al. (1998) showed that herring actively selected larger stages of both *C. hyperboreus* and *C. finmarchicus* compared to in situ densities of their stage distributions. And technicians specialized in fish stomach analyses at the Institute of Marine Research in Norway report that it is not unusual to find *C. hyperboreus* carcasses in stomach samples from pelagic fish in the Norwegian Sea (Herdis Langøy, pers. comm.). Also, individual *C. hyperboreus* can only be identified when the carcasses are whole and large compared to other calanoids, meaning that young stages may erroneously be placed as older stages of *C. finmarchicus*. Langøy et al. (2012) showed that "other copepods" (a category which comprises older stages of *C. hyperboreus*) and "unidentified copepod remains" together may constitute from 30% to over 60% of the total content in herring and mackerel stomachs from the Norwegian Sea. This suggests that the importance of *C. hyperboreus* in pelagic fishes' diet in the Norwegian Sea might have been underestimated so far.

Visual predation from pelagic and mesopelagic fish in the presented model are implemented assuming size-dependent selectivity and a temperature-dependent distribution of predators (linear increase in mortality from predation above 2.5 °C). This was however not sufficient to prevent the establishment of a *C. hyperboreus* population in the Norwegian Sea without a geographically defined increase in mortality rates. Based on the above, we feel confident that adding a fixed mortality for *C. hyperboreus* in the Norwegian Sea to some degree alleviates the shortcoming of the implemented predator field, and that low abundances of *C. hyperboreus* in this region is more likely driven by top-down control from predation rather than bottom-up limitations on growth. In this sense, the additional mortality rate could be modelled more realistically in future work by coupling it to estimates of annual stock size and spatial distribution patterns of pelagic fish, or including the pelagic fish IBMs in NORWECOM.E2E (e.g. Utne et al., 2012).

The main limitation of our study is the incomplete parameterization of the full *C. hyperboreus* life cycle, together with a lack of precise information on how to represent these in many cases poorly understood processes. Also, thorough sensitivity testing of model parameters has been difficult to perform merely due to the model's size and computational constraints when running 3D ecosystem models over a large area (initial and final distributions of the OWD, WUD and EDD genes are given as sensitivity information in the Appendix). We hope that new observations, experiments or other modelling approaches can help us improve some of the shortcomings of this model in the future. For instance, feeding is known to start at nauplii stage N3 (Jung-Madsen et al., 2013), however when implementing this the modelled stage development times did not agree with field observations. Therefore, it was chosen to use a Belhradek function parametrized from Jung-Madsen et al. (2013) and Conover (1967) for all stages from egg to C2. Also, *C. hyperboreus* spends most of the year in the deep, and what triggers the descent and ascent between deep- and surface waters is a large unknown. Building on a lipid-accumulation window hypothesis (e.g. Johnson et al., 2008) such as in the *C. finmarchicus* IBM (Hjøllo et al., 2012) was difficult to implement for a calanoid with multiple overwintering phases as *C. hyperboreus*, and we landed on a simpler but perhaps more unrealistic solution (fixed date within a given time window). This aspect should nevertheless be elaborated in future development of the model. Spawning in the model environment is limited in time (November 1 to April 1) but could be made dependent on environmental clues and/or previous life history. And are copepods in nature able to undergo diapause in the same stage two subsequent winters if their fats reserves can support this, or will their mortality increase due to slow growth? Furthermore, the role of ice-algae as food for *C. hyperboreus* arose as a key, unresolved question about this species. The step going from individuals to a full population model depends on model tuning. Mortality is almost impossible to measure *in situ*, thus a population model is the art of balancing reproduction, growth and longevity with different mortality terms such that the population neither goes extinct nor explodes. Jung-Madsen et al. (2013) report on a mortality of starving nauplii of 4 % d^{-1} which is comparable to our rate (Table 2). However, even if there are several environmentally dynamic terms in the modelled mortalities, it still depends on fixed individual rates; an assumption which is known to be wrong. As a full life cycle IBM integrates equations of mean observed behaviour of individuals that will take their own decisions based on earlier life history and local environmental impact, the modelled within-population variability will always be limited. Nevertheless, through the present study the *C. hyperboreus* IBM has shown its ability to represent this key zooplankton species and point at gaps in our understanding of its function in the ecosystem.

5. Concluding remarks

While observations give an incomplete access to a natural phenomenon, ecosystem models offer an incomplete representation or parameterization of processes and components of a natural system (Oreskes et al., 1994). In the present study an IBM is built from published knowledge of *C. hyperboreus* encompassing observed natural variations. In this context the model represents a framework where available information can be integrated and tested to disclose knowledge gaps and possible inconsistencies between independent studies and observational data sets. We have shown that individual variation in development and life cycle length may be a natural result from transportation through environmental gradients, which supports the large variation reported from observational studies. And the current knowledge of *C. hyperboreus* does not support that its distribution is structured by environmental control. The role of *C. hyperboreus* as food for planktivores in the highly productive the Norwegian Sea will be important to address for future studies, perhaps using quantitative DNA analyses on pelagic fish stomach samples. In the end, predicting how a warming climate will affect the base of the marine food chain will be central for our ability to project future states of marine ecosystems. But to be able to do so, we first need to validate our current understanding of the mechanisms structuring existing distributions and population dynamics. Synthesizing observational and experimental results in a modelling framework like our own is an important first step in this "knowledge validation".

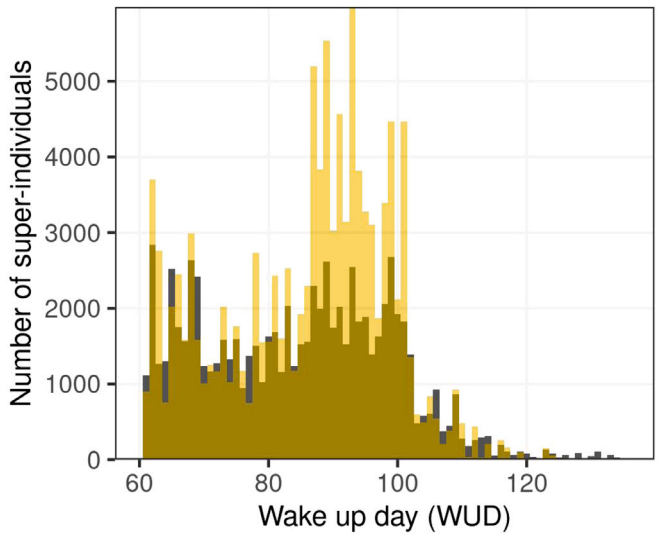

Fig. A.1. Frequency distribution of the wake-up-day (WUD) gene in the population of super-individuals at the start (grey) and end (transparent yellow) of the 25 years main simulation.

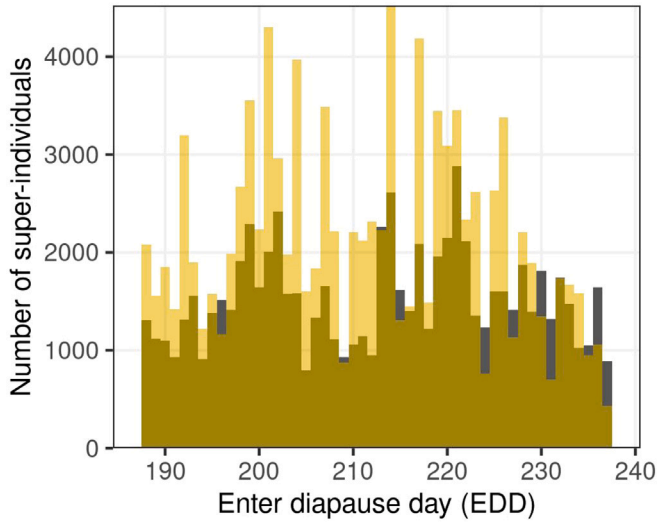

Fig. A.2. Frequency distribution of the enter-diapause-day (EDD) gene in the population of super-individuals at the start (grey) and end (transparent yellow) of the 25 years main simulation.

Declaration of competing interest

The authors declare that they have no known competing financial interests or personal relationships that could have appeared to influence the work reported in this paper.

Acknowledgements

The work resulting in this article was financed by the Institute of Marine Research, Bergen, Norway, and the Norwegian Research Council through the projects *ECCO* (RCN project no. 200508) and *The Nansen Legacy* (RCN project no. 276730).

Appendix

See Figs. A.1–A.3.

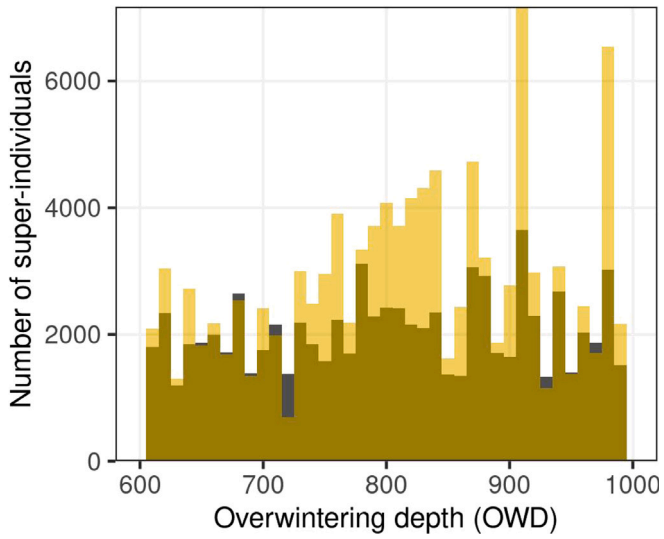

Fig. A.3. Frequency distribution of the overwintering depth (OWD) gene in the population of super-individuals at the start (grey) and end (transparent yellow) of the 25 years main simulation.

References

Aksnes, D., Blindheim, J., 1996. Circulation patterns in the north Atlantic and possible impact on population dynamics of *Calanus finmarchicus*. Ophelia 44, 7–28.

Aksnes, D., Ulvestad, K., Baliño, B., Berntsen, J., Egge, J., Svendsen, E., 1995. Ecological modelling in coastal waters: Towards predictive physical–chemical-biological simulation models. Ophelia 41, 5–36.

Aksnes, D.L., Utne, A.C.W., 1997. A revised model of visual range in fish. Sarsia 82 (2), 137–147.

Ashjian, C.J., Campbell, R.G., Welch, H.E., Butler, M., Van Keuren, D., 2003. Annual cycle in abundance, distribution, and size in relation to hydrography of important copepod species in the western Arctic Ocean. Deep Sea Res. I: Oceanogr. Res. Pap. 50 (10), 1235–1261.

Astthorsson, O.S., Gislason, A., 2003. Seasonal variations in abundance, development and vertical distribution of *Calanus finmarchicus*, *C. hyperboreus* and *C. glacialis* in the east Icelandic current. J. Plankton Res. 25 (7), 843–854.

Bachiller, E., Skaret, G., Nøttestad, L., Slotte, A., 2016. Feeding ecology of northeast Atlantic mackerel, Norwegian spring-spawning herring and blue whiting in the Norwegian sea. PLoS One 11 (2), e0149238.

Bode, A., Barquero, S., Gonzales, N., Alvarez-Ossorio, M., Varela, M., 2004. Contribution of heterotrophic plankton to nitrogen regeneration in the upwelling ecosystem of La Coruna (NW Spain). J. Plankton Res. 26 (1), 11–28.

Broms, C., Melle, W., Kaartvedt, S., 2009. Oceanic distribution and life cycle of *Calanus* species in the Norwegian Sea and adjacent waters. Deep Sea Res. II: Top. Stud. Oceanogr. 56, 1910–1921.

Budgell, W., 2005. Numerical simulation of ice-ocean variability in the Barents Sea region: Towards dynamical downscaling. Ocean Dyn. 55, 370–387.

Campbell, R.G., Sherr, E.B., Ashjian, C., Plourde, S., Sherr, B., Hill, V., Stockwell, D., 2009. Mesozooplankton prey preference and grazing impact in the western Arctic Ocean. Deep-Sea Res. II 56, 1274–1289.

Carlotti, F., Wolf, K.-U., 1998. A Lagrangian ensemble model of *Calanus finmarchicus* coupled with a 1-D ecosystem model. Fisheries Oceanography 7, 191–204.

Carstensen, J., Weydmann, A., Olszewska, A., Kwaśniewski, S., 2012. Effects of environmental conditions on the biomass of *Calanus spp.* in the Nordic seas. J. Plankton Res. 34 (11), 951–966.

Chambers, C., 1993. Phenotypic variability in fish populations and its representation in individual-based models. Trans. Am. Fish. Soc. 122, 404–414.

Choquet, M., Hatlebakk, M., Dhanasiri, A.K.S., Kosobokova, K., Smolina, I., Søreide, J.E., Svensen, C., Melle, W., Kwaśniewski, S., Eiane, K., Daase, M., Tverberg, V., Skreslet, S., Bucklin, A., Hoarau, G., 2017. Genetics redraws pelagic biogeography of *Calanus*. Biol. Lett. 13 (12), 20170588.

Conover, R., 1967. Reproductive cycle, early development, and fecundity in laboratory populations of the copepod *Calanus hyperboreus*. Crustaceana 13 (1), 61–72.

Conover, R.J., 1988. Comparative life histories in the genera *Calanus* and *Neocalanus* in high latitudes of the northern Hemisphere. Hydrobiologia 167 (1), 127–142.

Conover, R.J., Siferd, T.D., 1993. Dark-season survival strategies of coastal zone zooplankton in the Canadian Arctic. Arctic 46 (4), 303–311.

Daase, M., Eiane, K., Aksnes, D., Vogedes, D., 2008. Vertical distribution of *Calanus spp.* and *Metridia longa* at four Arctic locations. Mar. Biol. Res. 4 (3), 193–207.

Dale, T., Bagøien, E., Melle, W., Kaartvedt, S., 1999. Can predator avoidance explain varying overwintering depth of *Calanus* in different oceanic water masses? Mar. Ecol. Prog. Ser. 179, 113–121.

Dalpadado, P., Ellertsen, B., Melle, W., Dommasnes, A., 1998. Food and Feeding Conditions and Prey Selectivity of Herring (*Clupea Harengus*) Through Its Feeding Migrations from Coastal Areas of Norway to the Atlantic and Arctic Watermasses of the Nordic Seas. Tech. Rep. 2, ICES CM.

DeAngelis, D.L., Mooij, W.M., 2005. Individual-based modeling of ecological and evolutionary processes. Annu. Rev. Ecol. Evol. Syst. 36 (1), 147–168.

Diel, S., 1991. On the life history of dominant copepod species (*Calanus finmarchicus*, *C. glacialis*, *C. hyperboreus*, *Metridia longa*) in the Fram Strait. Rep. Polar Res. 88, 1–113.

Dorman, J.G., Sydeman, W.J., Bograd, S.J., Powell, T.M., 2015. An individual-based model of the krill *Euphausia pacifica* in the California current. Prog. Oceanogr. 138, 504–520.

Eiane, K., Aksnes, D.L., Ohman, M.D., Wood, S., Martinussen, M.B., 2002. Stage-specific mortality of *Calanus* spp. under different predation regimes. Limnol. Oceanogr. 47 (3), 636–645.

Falk-Petersen, S., Hop, H., Budgell, P., Hegseth, E., Korsnes, R., Løyning, T., Ørbek, J., Kawamura, T., Shirasawa, K., 2000. Physival and ecological proceses in the marginal ice zone of the northern Barents Sea during the summer melt period. J. Mar. Syst. 27, 131–159.

Falk-Petersen, S., Mayzaud, P., Kattner, G., Sargent, J., 2009. Lipids and life strategy of Arctic *Calanus*. Mar. Biol. Res. 5 (1), 18–39.

Fiksen, Ø., 2000. The adaptive timing of diapause - a search for evolutionarily robust strategies in *Calanus finmarchicus*. ICES J. Mar. Sci. 57, 1825–1833.

Gao, S., Hjøllo, S.S., Falkenhaug, T., Strand, E., Edwards, M., Skogen, M.D., 2021. Over-wintering distribution, inflow patterns and sustainability of *Calanus finmarchicus* in the North Sea. Prog. Oceanogr. 194, 102567.

Garber, J., 1984. Laboratory study of nitrogen and phosphorous remineralization during decomposition of coastal plankton and seston. Estuar. Coast. Shelf Sci. 16, 685–702.

Gehlen, M., Malschaert, H., Raaphorst, W., 1995. Spatial and temporal variability of benthic silica fluxes in the southeastern North Sea. Cont. Shelf Res. 13, 1675–1696.

Gislason, A., 2018. Life cycles and seasonal vertical distributions of copepods in the Iceland Sea. Polar Biol. 41 (12), 2575–2589.

Gjøsæter, H., Kawaguchi, K., 1980. A Review of the World Resources of Mesopelagic Fish. Tech. Rep. 193, FAO Technical Fisheries Reports.

Green, N., Heldal, H., Måge, A., Aas, W., Gafvert, T., Schrum, C., Boitsov, S., Breivik, K., Iosjpe, M., Yakushev, E., Skogen, M., Høgåsen, T., Eckhardt, S., Christiansen, A., Daae, K., Durand, D., Debloskaya, E., 2011. Tilførselsprogrammet 2010. Overvåking av Tilførsler og Miljøtilstand i Nordsjøen. Tech. Rep. TA 2810/2011, KLIF, Oslo, Norway, ISBN: 978-82-577-5922-3, 101 + 6 App.

Grimm, V., Berger, U., Bastiansen, F., Eliassen, S., Ginot, V., Giske, J., Goss-Custard, J., Grand, T., Heinz, S., Huse, G., Huth, A., Jepsen, J., Jørgensen, C., Mooij, W., Müller, B., Peer, G., Piou, C., Railsback, S., Robbins, A.M., Robbins, M., Rossmanith, E., Rüger, N., Strand, E., Souissi, S., Stillman, R., Vabø, R., Visser, U., DeAngelis, A., 2006. A standard protocol for describing individual-based and agent-based models. Ecol. Model. 198, 115–126.

Grimm, V., Berger, U., DeAngelis, D.L., Polhill, J.G., Giske, J., Railsback, S.F., 2010. The ODD protocol: A review and first update. Ecol. Model. 221 (23), 2760–2768.

Grimm, V., Railsback, S., 2005. Individual-Based Modeling and Ecology. University Press, Princeton.

Häfker, N.S., Teschke, M., Last, K.S., Pond, D.W., Hüppe, L., Meyer, B., 2018. *Calanus finmarchicus* seasonal cycle and diapause in relation to gene expression, physiology, and endogenous clocks. Limnol. Oceanogr. 63, 2815–2838.

Henriksen, M.V., Jung-Madsen, S., Nielsen, T.G., Møller, E.F., Henriksen, K.V., Markager, S., Hansen, B.W., 2012. Effects of temperature and food availability on feeding and egg production of *Calanus hyperboreus* from Disko Bay, Western Greenland. Mar. Ecol. Prog. Ser. 447, 109–126.

Hirche, H.-J., 1991. Distribution of dominant calanoid copepod species in the Greenland Sea during late fall. Polar Biol. 11 (6), 351–362.

Hirche, H.-J., 1997. Life cycle of the copepod *Calanus hyperboreus* in the Greenland Sea. Mar. Biol. 128, 607–618.

Hirche, H.-J., 2013. Long-term experiments on lifespan, reproductive activity and timing of reproduction in the Arctic copepod *Calanus hyperboreus*. Mar. Biol. 160, 2469–2481.

Hirche, H.-J., Muyakshin, S., Klages, M., Auel, H., 2006. Aggregation of the Arctic copepod *Calanus hyperboreus* over the ocean floor of the Greenland Sea. Deep Sea Res. I: Oceanogr. Res. Pap. 53 (2), 310–320.

Hirche, H.-J., Niehoff, B., 1996. Reproduction of the Arctic copepod *Calanus hyperboreus* in the Greenland Sea-field and laboratory observations. Polar Biol. 16, 209–219.

Hjøllo, S.S., Hansen, C., Skogen, M.D., 2021. Assessing the importance of zooplankton sampling patterns with an ecosystem model. Mar. Ecol. Prog. Ser. DYNMODav1.

Hjøllo, S., Huse, G., Skogen, M.D., Melle, W., 2012. Modelling secondary production in the Norwegian Sea with a fully coupled physical/primary production/individual-based *Calanus finmarchicus* model system. Mar. Biol. Res. 8 (5–6), 508–526.

Huse, G., Melle, W., Skogen, M., Hjøllo, S., Svendsen, E., Budgell, W., 2018. Modeling emergent life histories of copepods. Front. Ecol. Evol. 6, 23.

Huse, G., Strand, E., Giske, J., 1999. Implementing behaviour in individual-based models using neural networks and genetic algorithms. Evol. Ecol. 13, 469–483.

ICES, 2020. Working group on widely distributed stocks (WGWIDE). ICES Sci. Rep. 2 (82), 1019.

Ji, R., Ashjian, C.J., Campbell, R.G., Chen, C., Gao, G., Davis, C.S., Cowles, G.W., Beardsley, R.C., 2012. Life history and biogeography of *Calanus* copepods in the Arctic Ocean: An individual-based modeling study. Prog. Oceanogr. 96 (1), 40–56.

Johnson, C.L., Leising, A.W., Runge, J.A., Head, E.J.H., Pepin, P., Plourde, S., Durbin, E.G., 2008. Characteristics of *Calanus finmarchicus* dormancy patterns in the northwest Atlantic. ICES J. Mar. Sci. 65 (3), 339–350.

Jung-Madsen, S., Nielsen, T., Grønkjær, P., Hansen, B., Møller, E., 2013. Early development of *Calanus hyperboreus* nauplii: Response to a changing ocean. Limnol. Oceanogr. 58 (6), 2109–2121.

Kaartvedt, S., 2000. Life history of *Calanus finmarchicus* in the Norwegian Sea in relation to planktivorous fish. ICES J. Mar. Sci. 57 (6), 1819–1824.

Klevjer, T.A., Melle, W., Knutsen, T., Aksnes, D.L., 2020. Vertical distribution and migration of mesopelagic scatterers in four north Atlantic basins. Deep Sea Res. II: Top. Stud. Oceanogr. 180, 104811.

Kvile, K.Ø., Ashjian, C., Feng, Z., Zhang, J., Ji, R., 2018. Pushing the limit: Resilience of an Arctic copepod to environmental fluctuations. Global Change Biol. 24 (11), 5426–5439.

Langøy, H., Nøttestad, L., Skaret, G., Broms, C., Fernö, A., 2012. Overlap in distribution and diets of atlantic mackerel (*Scomber scombrus*), Norwegian spring-spawning herring (*Clupea harengus*) and blue whiting (*Micromesistius poutassou*) in the Norwegian Sea during late summer. Mar. Biol. Res. 8 (5), 442–460.

Lien, V., Budgell, P., Ådlandsvik, B., Svendsen, E., 2006. Validating Results from the Model Roms, with Respect To Volume Transports and Heat Fluxes in the Nordic Seas. Tech. Rep. Fisken og Havet 2/2006, Institute of Marine Research, Bergen, Norway.

Lohse, L., Kloostechuis, H., Raaphorst, W., Helder, W., 1996. Denitrification rates as measured by the isotope pairing method and by the acetylene inhiluition technique in continental shelf sediments of the North Sea. Mar. Ecol. Prog. Ser. 132, 169–179.

Lohse, L., Malschaert, F., Slomp, C., Helder, W., Raaphorst, W., 1995. Sediment-water fluxes of inorganic nitrogen compounds along the transport route of organic matter in the North Sea. Ophelia 41, 173–197.

Maps, F., Record, N.R., Pershing, A.J., 2014. A metabolic approach to dormancy in pelagic copepods helps explaining inter- and intra-specific variability in life-history strategies. J. Plankton Res. 36 (1), 18–30.

Martinsen, E., Engedahl, H., 1987. Implementation and testing of a lateral boundary scheme as an open boundary condition in a barotropic ocean model. Coast. Eng. 11, 603–627.

Mayer, B., 1995. Ein Dreidimensionales, Numerisches Schwebstoff-Transportmodell Mit Anwendung Auf Die Deutsche Bucht. Tech. Rep. GKSS 95/E/59, GKSS-Forschungszentrum Geesthacht GmbH, (ISSN: 0344-9629) p. 104.

McLaren, I.A., Sevigny, J.M., Corkett, C.J., 1988. Body sizes, development rates, and genome sizes among *Calanus* species. Hydrobiologia 167 (1), 275–284.

Misund, O.A., Vilhjálmsson, H., Jákupsstovu, S.H., Røttingen, I., Belikov, S., Asthorsson, O., Blindheim, J., Jónsson, J., Krysov, A., Malmberg, S.A., Sveinbjórnsson, S., 1998. Distribution, migration and abundance of Norwegian spring-spawning herring in relation to the temperature and zooplankton biomass in the Norwegian Sea as recorded by coordinated surveys in spring and summer 1996. Sarsia 83 (2), 117–127.

Moll, A., Stegert, C., 2007. Modeling *Pseudocalanus elongatus* population dynamics embedded in a water column ecosystem model for the northern North Sea. J. Mar. Syst. 64 (1–4), 35–46.

Møller, E.F., Nielsen, T.G., Richardson, K., 2006. The zooplankton community in the Greenland Sea: Composition and role in carbon turnover. Deep Sea Res. I: Oceanogr. Res. Pap. 53 (1), 76–93.

Mork, K.A., Blindheim, J., 2000. Variations in the Atlantic inflow to the Nordic Seas, 1955–1996. Deep Sea Res. I: Oceanogr. Res. Pap. 47 (6), 1035–1057.

Niehoff, B., Madsen, S., Hansen, B., Nielsen, T., 2002. Reproductive cycles of three dominant *Calanus* species in Disko Bay, west Greenland. Mar. Biol. 140 (3), 567–576.

Ohman, M.D., Romagnan, J.-B., 2016. Nonlinear effects of body size and optical attenuation on diel vertical migration by zooplankton. Limnol. Oceanogr. 61 (2), 765–770.

Olafsdottir, A.H., Utne, K.R., Jacobsen, J.A., Jansen, T., Óskarsson, G.J., Nøttestad, L., Elvarsson, B., Broms, C., Slotte, A., 2019. Geographical expansion of northeast Atlantic mackerel (*Scomber scombrus*) in the Nordic seas from 2007 to 2016 was primarily driven by stock size and constrained by low temperatures. Deep Sea Res. II: Top. Stud. Oceanogr. 159, 152–168.

Oreskes, N., Shrader-Frechette, K., Belitz, K., 1994. Verification, validation and confirmation of numerical models in the earth sciences. Science 263 (5147), 641–646.

Østvedt, O., 1955. Zooplankton investigations from weather ship M in the Norwegian Sea. In: Hvalrådets Skrifter. Scientific Results of Marine Biological Research. pp. 1–93.

Pätsch, J., Kühn, W., Moll, A.H.L., 2009. ECOHAM4 User Guide - ECOSystem Model, HAMBurg, Version 4. Tech. Rep. 01-2009, Institut für Meereskunde, Hamburg, Germany.

Plourde, S., Joly, P., Runge, J.A., Dodson, J., Zakardjian, B., 2003. Life cycle of *Calanus hyperboreus* in the lower St. Lawrence estuary and its relationship to local environmental conditions. Mar. Ecol. Prog. Ser. 255, 219–233.

Pohlmann, T., Puls, W., 1994. Currents and transport in water. In: Sündermann, J. (Ed.), Circulation and Contaminant Fluxes in the North Sea. Springer Verlag, Berlin, pp. 345–402.

Renaud, P.E., Daase, M., Banas, N.S., Gabrielsen, T.M., Søreide, J.E., Ø, Varpe., Cottier, F., Falk-Petersen, S., Halsband, C., Vogedes, D., Heggland, K., Berge, J., 2018. Pelagic food-webs in a changing Arctic: A trait-based perspective suggests a mode of resilience. ICES J. Mar. Sci. 75 (6), 1871–1881.

Rey, F., 2004. Phytoplankton: the grass of the sea. In: Skjoldal, H.R. (Ed.), The Norwegian Sea Ecosystem. Tapir Academic Press, pp. 329–344.

Richardson, K., Markager, S., Buch, E., Lassen, M., Kristensen, A., 2005. Seasonal distribution of primary production, phytoplankton biomass and size distribution in the Greenland Sea. Deep-Sea Res. I 52, 979–999.

Sainmont, J., Andersen, K.H., Varpe, Ø., Visser, A.W., 2014. Capital versus income breeding in a seasonal environment. Amer. Nat. 184 (4), 466–476.

Scheffer, M., Baveco, J., de Angelis, D., Rose, K., van Nes, E., 1995. Super individuals a simple solution for modelling large populations on an individual basis. Ecol. Model. 80, 161–170.

Scott, C., Kwasniewski, S., Falk-Petersen, S., Sargant, J., 2000. Lipids and life strategies of *Calanus finmarchicus*, *Calanus glacialis* and *Calanus hyperboreus* in late autumn, Kongsfjorden, Svalbard. Polar Biol. 23, 510–516.

Shchepetkin, A., McWilliams, J., 2005. The regional oceanic modeling system (ROMS): a split-explicit, free-surface, topography-following-coordinate oceanic model. Ocean Model. 9, 347–404.

Skaret, G., Dalpadado, P., Hjøllo, S., Skogen, M., Strand, E., 2014. *Calanus finmarchicus* abundance, production and population dynamics in the Barents Sea in a future climate. Prog. Oceanogr. 125, 26–39.

Skartveit, A., Olseth, J.A., 1986. Modelling slope irradiance at high lattitudes. Sol. Energy 36 (4), 333–344.

Skartveit, A., Olseth, J.A., 1987. A model for the diffuse fraction of hourly global radiation. Sol. Energy 37, 271–274.

Skjoldal, H., 2004. The Norwegian Sea Ecosystem. Tapir Academic Press, Trondheim, Norway, p. 559.

Skogen, M., Budgell, W., Rey, F., 2007. Interannual variability in Nordic Seas primary production. ICES J. Mar. Sci. 64, 889–898.

Skogen, M., Hjøllo, S., Sandø, A., Tjiputra, J., 2018. Future ecosystem changes in the north east Atlantic: a comparison between a global and a regional model system. ICES J. Mar. Sci. 75 (7), 2355–2369.

Skogen, M., Olsen, A., Børsheim, K., Sandø, A., Skjelvan, I., 2014. Modelling ocean acidification in the Nordic and Barents Seas in present and future climate. J. Mar. Syst. 131, 10–20.

Skogen, M., Svendsen, E., Berntsen, J., Aksnes, D., Ulvestad, K., 1995. Modelling the primary production in the North Sea using a coupled 3 dimensional physical chemical biological ocean model. Estuar. Coast. Shelf Sci. 41, 545–565.

Søreide, J.E., Falk-Petersen, S., Hegseth, E.N., Hop, H., Carroll, M.L., Hobson, K.A., Blachowiak-Samolyk, K., 2008. Seasonal feeding strategies of *Calanus* in the high-Arctic Svalbard region. Deep-Sea Res. II: Top. Stud. Oceanogr. 55 (20–21), 2225–2244.

Søreide, J.E., Leu, E., Berge, J., Graeve, M., Falk-Petersen, S., 2010. Timing of blooms, algal food quality and *Calanus glacialis* reproduction and growth in a changing Arctic. Global Change Biol. 16 (11), 3154–3163.

Stegert, C., Moll, A., Kreus, M., 2009. Validation of the three-dimensional ECOHAM model in the German bight for 2004 including population dynamics of *Pseudocalnus elongatus*. J. Sea Res. 62, 1–15.

Stillman, R.A., Railsback, S.F., Giske, J., Berger, U., Grimm, V., 2015. Making predictions in a changing world: The benefits of individual-based ecology. BioScience 65 (2), 140–150.

Strand, E., Bagøien, E., Edwards, M., Broms, C., Klevjer, T., 2020. Spatial distributions and seasonality of four *Calanus* species in the Northeast Atlantic. Prog. Oceanogr. 185, 102344.

Utne, K., Hjøllo, S., Huse, G., Skogen, M., 2012. Estimating consumption of *Calanus finmarchicus* by planktivorous fish in the Norwegian Sea using a fully coupled 3D model system. Mar. Biol. Res. 8 (5–6), 527–547.

van Deurs, M., Jørgensen, C., Fiksen, Ø., 2015. Effects of copepod size on fish growth: a model based on data for North Sea sandeel. Mar. Ecol. Prog. Ser. 520, 235–243.

Visser, A., Grønning, J., Jonasdottir, S., 2017. *Calanus hyperboreus* and the lipid pump. Limnol. Oceanogr. 62, 1155–1165.

Xu, Y., Rose, K.A., Chai, F., Chavez, F.P., Ayon, P., 2015. Does spatial variation in environmental conditions affect recruitment? A study using a 3-D model of Peruvian anchovy. Prog. Oceanogr. 138, 417–430.